Optics Communications 482 (2021) 126597

Contents lists available at ScienceDirect

Optics Communications

journal homepage: www.elsevier.com/locate/optcom

Simulation analysis and comparison of the effects of aberrations on multiphoton fluorescent light sheets

Wenqiang Sun [a,b], Nan Li [a,b], Caihua Zhang [a,b], Quanquan Mu [a,*], Xingyun Zhang [a,*], Chengliang Yang [a,b], Zenghui Peng [a,b], Zhihui Diao [a,b], Li Xuan [a], Lina Shao [b,c]

[a] State Key Laboratory of Applied Optics, Changchun Institute of Optics, Fine Mechanics and Physics, Chinese Academy of Sciences, Changchun, Jilin, 130033, China

[b] University of Chinese Academy of Sciences, Beijing, 100049, China

[c] State Key Laboratory of Electroanalytical Chemistry, Changchun Institute of Applied Chemistry, Chinese Academy of Sciences, Changchun, Jilin 130022, China

ARTICLE INFO

Keywords:
Aberration correction
Multi-photon light sheet
Adaptive optics

ABSTRACT

Multi-photon scanning light-sheet microscope, which combines the advantages of light-sheet illumination and multi-photon excitation, has high axial resolution, low photobleaching, and a large field of view. However, as the light sheet goes deeper into the biological tissue, biological optical aberrations caused by the uneven refractive index inside the organism become non-negligible factors that dramatically increase the thickness and decrease the light intensity of the light sheet. This paper theoretically deduces and simulates the influence of aberrations on the intensity and thickness of the two-, three-, and four-photon fluorescent light sheet. A clear general trend is obvious. With the increasing amplitude of aberration, the effect of aberration on the light sheet thickness and intensity increases in each multiphoton light sheet. In terms of thickness, the impact of high-order aberrations diminishes from the two-photon to the four-photon light sheet. However, in terms of intensity, the impact of high-order aberrations increases from the two-photon to the four-photon light sheet. The number of items to be corrected for each multiphoton light sheet is given and compared under random aberrations with different amplitudes. The results provide important guidance for the design and evaluation of adaptive optics in multi-photon light sheet microscopes.

1. Introduction

Selective Plane Illumination Microscopy has received much attention and has been rapidly developed since its appearance in 2004 [1]. Its imaging and illumination optical paths are separated orthogonally; its lateral illumination nature has the advantages of fast imaging speed and strong layer cutting ability. In 2008 [2], Keller et al. developed beam scanning light-sheet micro-imaging technology, which produces a more flexible and changeable light sheet. With the development of the multi-photon fluorescence excitation technology, multi-photon scanning light-sheet microscope has emerged; this microscope combines light-sheet illumination structure and multi-photon excitation [3,4]. It has the advantages of high-speed and long-term imaging in a large field of view; it is constantly developing from a two-photon light sheet to a three-photon light sheet and even a four-photon light sheet in the future in pursuit of deeper biological imaging. As the light sheet goes deeper into the biological tissue, biological optical aberrations become non-negligible factors that dramatically increase the thickness and decrease the light intensity of the light sheet, thereby reducing the resolution and field of view of the microscope [5].

To eliminate the impact of biological aberrations and improve the performance of the microscope, adaptive optics that could detect and correct optical aberrations in real time are widely used in various types of fluorescence microscopes [6], such as wide field microscope [7], confocal microscope [8], super resolution microscope [9], and single-photon light sheet microscope [10]. The effects of biological aberrations on a multiphoton light sheet are totally different from their effects on a single-photon light sheet because of the nonlinear feature and the light-sheet illumination structure. Thus, before designing a reasonable adaptive optics system for a nonlinear multiphoton light sheet illumination system, conducting a quantitative analysis of the effects of biological aberrations on the thickness and intensity of the nonlinear multiphoton light sheet is necessary. Sinefeld, D. and others [11] compared the effects of aberrations on the intensity of nonlinear multiphoton microscopes. In our previous work [12], we specifically conducted simulation studies to determine the effects of aberrations on two-photon light sheet fluorescence microscopes. Based on the results of the abovementioned studies, this paper focuses on the effects of aberrations on the quality of two-, three-, and four-photon fluorescent light sheets, including the changes in thickness

* Corresponding authors.
E-mail addresses: muquanquan@ciomp.ac.cn (Q. Mu), xyzhang@ciomp.ac.cn (X. Zhang).

https://doi.org/10.1016/j.optcom.2020.126597
Received 11 August 2020; Received in revised form 21 October 2020; Accepted 8 November 2020
Available online 11 November 2020

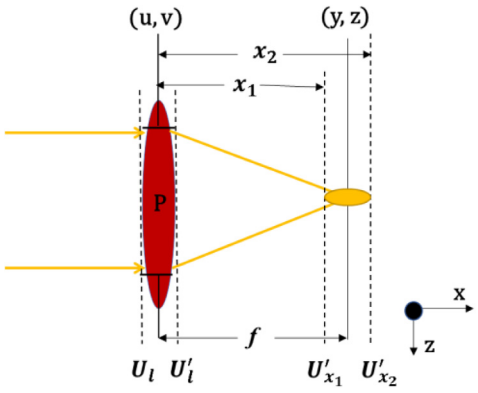

Fig. 1. The sketch map of light focused by a converging lens.

and intensity. Moreover, this paper discusses the necessity, similarities, and differences of adaptive optics for different multiphoton light sheet microscopes and also gives guidance for the design of an adaptive optics system for these microscopes.

2. Methods

2.1. Formation of multi-photon light sheet

Previously, we deduced the formation of two-photon light sheet theoretically [12]. In the current work, we expand to general multi-photon light sheet using similar methods. To simulate the effect of beam aberrations on the Nth nonlinear process, the aberration expressed in Zernike form was used to calculate the axial optical field distribution in the beam transmission process, and the axial scanning integral was performed for the Nth power intensity distribution. The details are as follows [13]:

The incident light is focused by using objective lens with focal length f, as shown in Fig. 1. The complex amplitude distribution $U'_l(u, v)$ behind the lens can be written as follows:

$$U'_l(u,v) = U_l(u,v)P(u,v)e^{i\phi(u,v)}\exp[-j\frac{k}{2f}(u^2+v^2)] \tag{1}$$

where U_l (u,v) is the complex amplitude disturbance incident on the lens, Φ (u, v) is the aberrations in the pupil plane, and $P(u,v)$ is the pupil function.

According to the Fresnel diffraction formula, the complex amplitude distribution U_x (y, z) near the focal plane of the lens can be written as follows:

$$U_x(y,z) = \frac{\exp[j\frac{k}{2x}(y^2+z^2)]}{j\lambda x} \times \iint U'_l(u,v)\exp[j\frac{k}{2x}(u^2+v^2)] \times \exp[-j\frac{2\pi}{\lambda x}(uy+vz)]dudv \tag{2}$$

where x is the distance from the lens to the imaging plane. A constant phase factor has been dropped.

By changing the distance x from x_1 to x_2, we obtain the complex amplitude distribution of the focus point along the x-axis. Then, the intensity distribution can be written as follows:

$$I_{x_1\to x_2} = U_{x_1\to x_2}(y,z) \times U_{x_1\to x_2}(y,z)^* \tag{3}$$

For the multi-photon excitation, the intensity of the detected fluorescence is as follows:

$$I_f = \kappa_n\delta_n\eta_n I^n \quad (n=2,3,4) \tag{4}$$

where κ_n is the collection efficiency of the imaging device, δ_n is the multi-photon cross-section, and η_n is the fluorescence quantum efficiency. $n = 2, 3, 4$ represents two-, three-, and four-photon excitation, respectively. Thus, the 3D effective multi-photon illumination point spread function PSF_{ill} can be expressed as follows:

$$PSF_{ill}(x,y,z) = \kappa\delta_n\eta_n {I^n}_{x_1\to x_2}(n=2,3,4) \tag{5}$$

After considering the effect of the detection camera, the intensity is integrated along the y-axis:

$$I_{camera}(x,z) = \int PSF_{ill}(x,y,z)dy \tag{6}$$

The virtual light sheet is scanned along the x-axis, and the intensity distribution of the multiphoton light sheet can be written as follows:

$$I_{light-sheet}(z) = \int I_{camera}(x,z)dx = \iint PSF_{ill}(x,y,z)dydx \tag{7}$$

2.2. Light sheet quality parameters

In a light sheet microscope, the thickness of the light sheet determines the layering ability of the system, and the intensity of light determines the depth of illumination. The effect of aberrations is reflected in the increasing thickness and the decreasing light intensity of the light sheet, which affect the performance of the system, as shown in Fig. 2. The distribution of illumination laser intensity (PSF_{ill}) along the beam propagation direction (x-axis) is simulated according to the Fourier transforming properties of a converging lens with no aberration, as shown in Fig. 2(a), and with the random aberration whose peak to valley (PV) and root mean square (RMS) of the aberrated wavefront are 1.5 μm and 0.2 μm, as shown in Fig. 2(b). The PSF_{ill} is distorted, the thickness of the generated light sheet is increased, and the intensity of fluorescence is decreased dramatically due to the effect of the aberration, as shown in Fig. 2(b). To quantify the influence of aberrations, we set parameters to evaluate the influence of aberrations on the light sheet thickness and intensity.

We used the same evaluation parameters mentioned in our previous article [10]. We set TR as a parameter to measure the effect of aberrations on the light sheet thickness. TR is the ratio between aberrated thickness (T_A) and aberration-free thickness (T_0) of the multiphoton light sheet, as follows:

$$TR = \frac{T_A}{T_O} \tag{8}$$

The full width at half maximum (FWHM) of the intensity distribution inaccurately describes the thickness of the aberrated light sheet. Because the distribution curve of intensity may be distorted. Thus, we define a new parameter T as the thickness of light sheet. The parameter T is the minimum width at 70% integral intensity of the cross-sectional energy of the thickness of the distorted light sheet, as shown in Fig. 3, and is equal to the FWHM of the two-photon light sheet in an aberration-free system. Then the thickness of the aberrated light sheet in biological specimens can be indicated accurately.

If TR equals 1, then no aberration is present. A large TR value indicates a greater light sheet thickness caused by the aberrations and the greater influence of the aberrations. Similarly, to measure the influence of aberrations on the intensity of light sheet, IR is set as the ratio of the highest intensity value with aberration influence (I_A) divided by the corresponding highest intensity value without aberration influence (I_O), as follows:

$$IR = \frac{I_A}{I_O} \tag{9}$$

The ideal value of IR is 1. A smaller IR value indicates a lower light sheet maximum intensity value caused by aberrations and the greater influence of the aberrations.

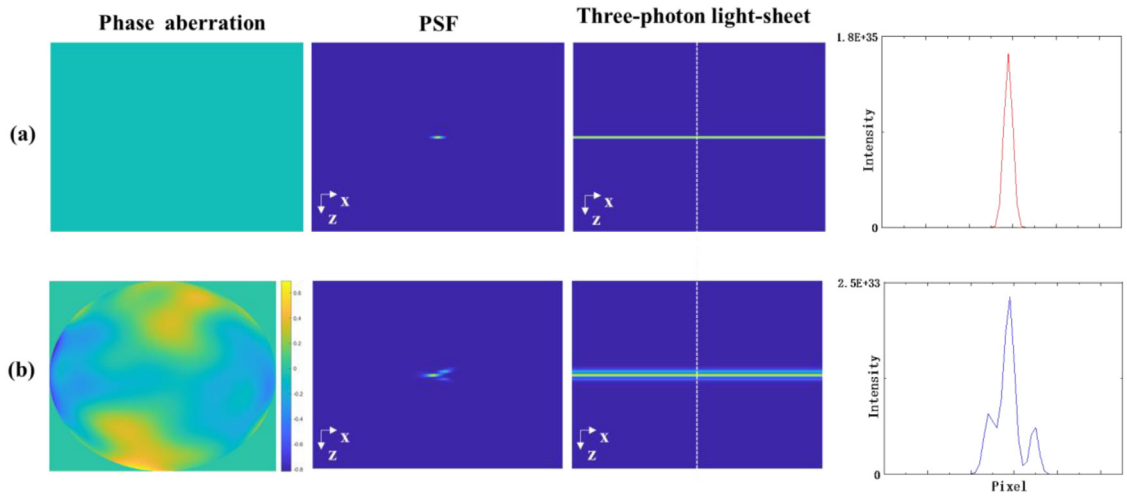

Fig. 2. The three-photon light-sheet simulation: (a) aberration-free phase, PSF_{ill}, and light sheet intensity distribution of the three-photon light sheets along the z-axis; (b) aberrated phase, PSF_{ill}, and light sheet intensity distribution of the three-photon light sheets along the z-axis.

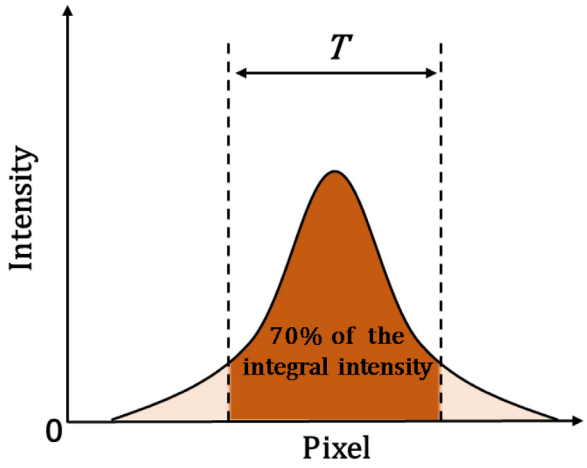

Fig. 3. Definition of the thickness T.

3. Results

Using the abovementioned numerical simulation method and the quantitative evaluation parameters, the effects of each Zernike mode aberration and random biological aberrations on the two-, three-, and four-photon fluorescent light sheets can be effectively simulated and analyzed.

In the simulation, the equivalent focal length (f) of the objective is set to 5 mm. The wavelength of the femtosecond pulse laser is set to 1000 nm. The effective aperture can be changed to obtain a flexible number aperture. The tip/tilt and defocus aberrations only affect the light sheet position and have no effect on the light sheet thickness and light intensity. Therefore, TR and IR remain the ideal values of 1 with tip/tilt and defocus aberrations and can be used for verification.

3.1. Effects of each Zernike mode

Zernike aberrations of different amplitudes and modes have different effects on the light sheets, and the same aberrations have different effects on varying light sheets (two-, three-, or four-photon). To analyze these two differences quantitatively, we simulate the influence of the first 104 Zernike aberrations on each multiphoton light sheet. The order of Zernike mode is given in Fig. 4. For each trial, a series of amplitudes of each aberration mode in the range of 0.1–2 wavelength is simulated. The result of the aberration influence is shown in Fig. 5.

First, the effects of different amplitudes and modes of aberrations on each multiphoton light sheet are studied. For each multiphoton light sheet, three representative simulation results are shown in Fig. 4((a)(b)(c)). For all the multiphoton light sheets, TR keeps increasing, and IR keeps decreasing with increasing amplitude of the aberration. Thus, the light sheet thickness increases sharply, and the light intensity decreases sharply. A larger aberration amplitude indicates greater damage to the quality of the multiphoton light sheet.

The aberrations of different modes have different influences under the same amplitude. Compared with the aberrations of other modes, low-order astigmatism ($N = 4, 6$) and the Zernike aberrations of modes whose angular frequency l is not equal to zero and a radial order n that is not equal to the absolute of the angular frequency l have a more serious effect. This seems to be a common law for all light sheets (two-, three-, and four-photon).

We study the different influence of the same aberration on each multi-photon light sheet (two-, three-, and four-photon). We first observe the different influences of the aberrations in Fig. 5((a)(b)(c)). In terms of the influence on thickness, TR that is affected by higher-order aberrations gets closer to 1 from the two-photon to the four-photon light sheet. Thus, the higher-order nonlinear optical sheet has a stronger suppression effect on the influence of higher-order aberrations on thickness.

We provide a more obvious representative comparison result in Fig. 5(d) of the effect of each multiphoton light sheet under the same aberration conditions. The PV of the amplitude of the same Zernike mode aberration is 1.5 wavelength. In terms of thickness, the impact of high-order aberrations diminishes from the two-photon to the four-photon light sheet.

In terms of intensity, the IR value becomes smaller under the same aberrations with increasing number of photons. This finding means that the light intensity drops faster and that the intensity of the higher-order nonlinear optical sheet is more seriously affected by the same aberrations.

In summary, greater aberrations have a much stronger impact on each multiphoton light sheet's thickness and light intensity. Low-order astigmatism ($N = 4, 6$) and the Zernike aberrations of those modes whose angular frequency l is not equal to zero and the radial order n that is not equal to the absolute of the angular frequency l have a greater impact than any other Zernike mode aberration. With increasing number of photons, the effect of higher-order Zernike aberrations on the thickness weakens, and the effect of each Zernike mode aberrations on light intensity becomes more serious.

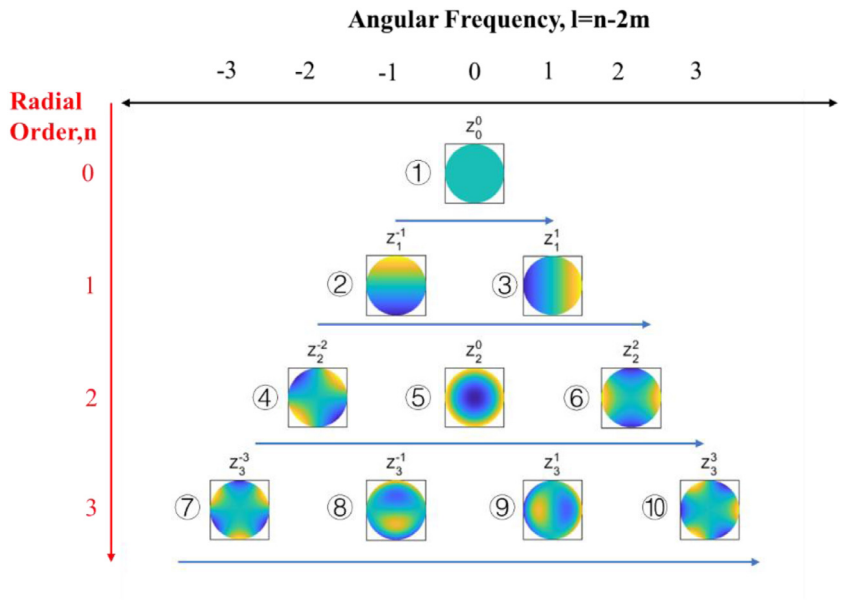

Fig. 4. Schematic diagram of Zernike mode Z_n^l simulation sequence. The number of N items starts from left to right, and the mode of the piston is N = 1. The index n represents the Zernike radial order, and l is the Zernike azimuthal order.

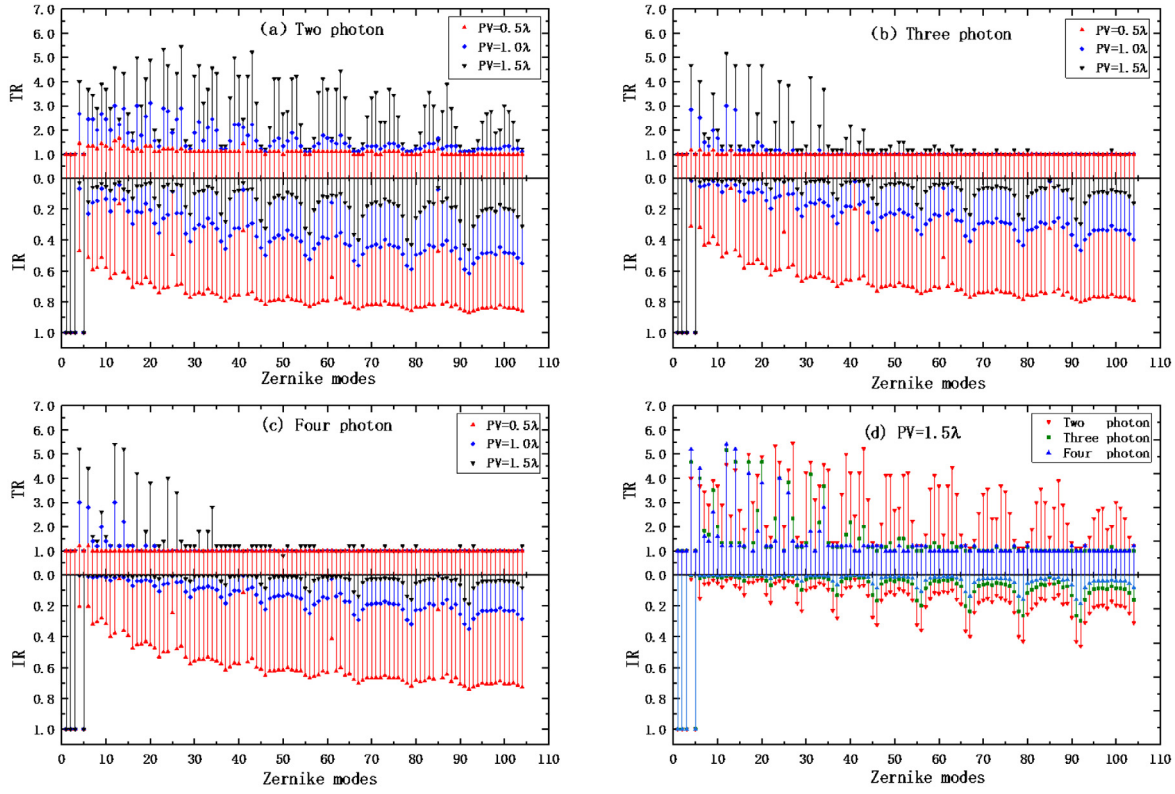

Fig. 5. Relationship between TR/IR and each Zernike mode in (a) two-, (b) three-, and (c) four-photon light sheet microscopes. (d) Comparison between TR/IR and each Zernike mode in two-, three-, and four-photon light sheet microscopes under the same PV = 1.5λ distorted aberration.

3.2. Effects of random biological aberrations

We study the effects and differences of biological random aberrations on multi-photon light sheets. First, we need to understand the characteristics of biological random aberrations to more realistically simulate the effects of biological aberrations. The aberration model in biological samples proposed by Schwertner et al. [14,15] shows that the aberration caused by the change in the refractive index of the biological sample can be approximated by random aberrations. Zernike modal standard deviation decreases with increasing order, and this general behavior is found in all samples. At each random aberration wavefront, the amplitude of the high-order Zernike mode is smaller than that of the low-order Zernike mode in general. We focus on how many low-order random biological aberrations need to be corrected to restore the quality of each multiphoton light sheet to a level close to the ideal one. According to the experimental results of Kai Wang et al. [16,17] on zebrafish embryo and mouse cortex, the aberrations of the biological sample from the surface layer to the deep layer (>500 μm) gradually

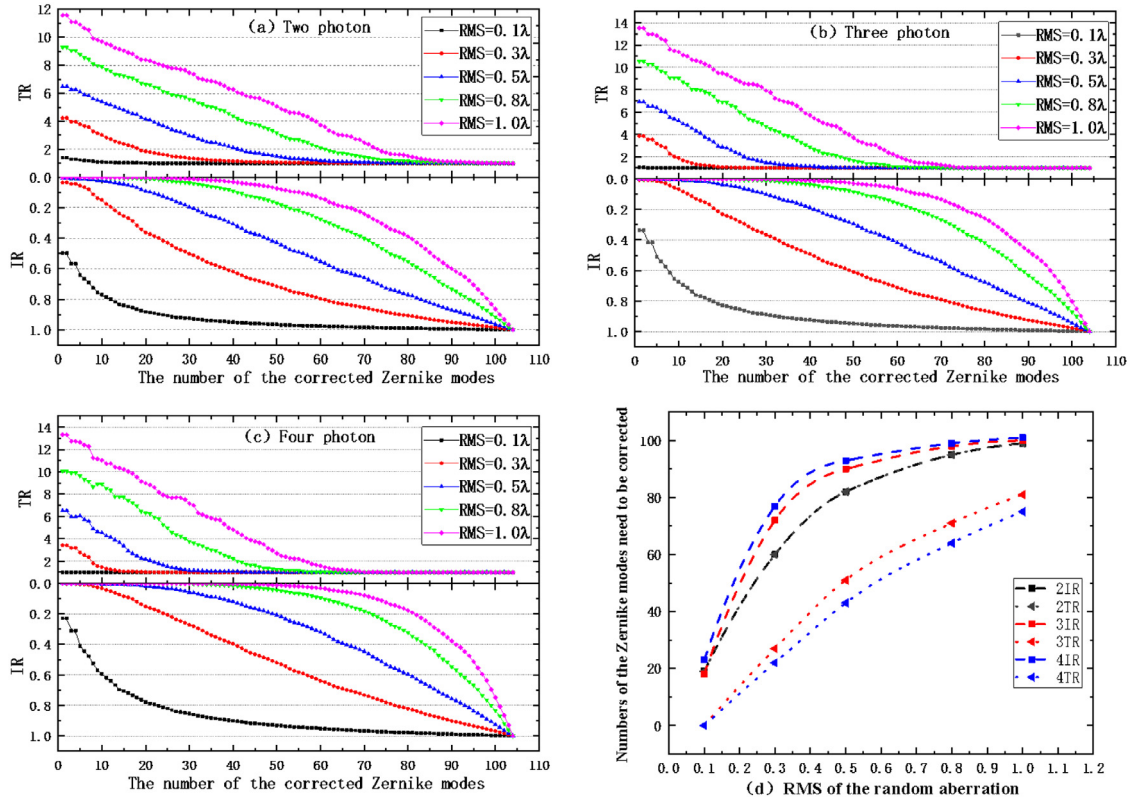

Fig. 6. TR/IR of different RMS of the initial random aberration varying with the number of corrected Zernike modes in (a) two-, (b) three-, and (c) four-photon light sheet. (d) Comparison of the number of correction terms corresponding to TR = 1.01 and IR = 0.8 in each photon light sheet with increasing RMS. The NA of the illumination objective is 0.8.

increased from RMS 0.1λ (λ = 1000 nm) to RMS1.0λ. Thus, we use RMS to indicate the intensity of random aberrations caused by the sample at different depths, and the variation ranges from 0.1λ to 1.0λ. According to the abovementioned aberration model, each aberration intensity randomly generates 1000 wavefronts, and the average TR and IR of 1000 groups of wavefronts are used to obtain the statistical results. The closer the TR and IR values are to 1, the better the correction effect is. Each multiphoton light sheet uses the same random aberrations. Fig. 6((a)(b)(c)) show the relationship between the corrected number of Zernike modes J under the same random aberrations of variable intensity and TR and IR in each multiphoton light sheet.

When TR = 1.01 and IR = 0.8, the light sheet quality is considered to be close to the ideal quality of the light sheet, thereby indicating the number of correction items corresponding to each multi-photon light sheet at different RMS aberrations. The result of a comparison is shown in Fig. 6(d).

First, the number of Zernike modes that need to be corrected in each multi-photon light sheet increases with increasing RMS of biological aberration. Second, we conclude that under the influence of aberrations at the same amplitude, the number of Zernike modes that need to be corrected in a two-photon light sheet maintains synchronization in terms of thickness and intensity. However, the correction terms of the intensity and thickness of higher-order nonlinearity are inconsistent. Furthermore, in terms of the influence of thickness on high-order nonlinear light sheet, the number of items that need to be corrected is reduced from the two-photon to the four-photon light sheet, but according to intensity, the number of items that need to be corrected is increased from the two-photon to the four-photon light sheet.

4. Discussion

The influence of the different amplitudes and characteristics of Zernike aberrations on each multi-photon light sheet is studied, and the difference in the influence of the same size and characteristics of the aberration between different multi-photon (two-, three-, or four-photon) light sheet is also obtained. The number of correction items required for random biological aberrations in each multiphoton light sheet is studied, and the difference in the number of correction items for each multiphoton light sheet with the same aberration is obtained.

Based on the abovementioned relationship, a series of results can be obtained. First, as the aberration increases, regardless of the PV of each Zernike mode or the RMS of the random biological Zernike modes, the impacts of aberrations on the thickness and the intensity and the Zernike modes that need to be corrected in each multiphoton light sheet increase. Second, the trends of the impacts of aberrations on the thickness and the intensity in multi-photon light sheet differ. Furthermore, in terms of thickness, the impact of high-order aberrations diminishes from the two-photon to the four-photon light sheet. However, in terms of intensity, the impact of each aberration increases from the two-photon to the four-photon light sheet.

The abovementioned results can provide suggestions for designing an adaptive multiphoton light sheet illumination microscopy system. First, the greater the aberrations are, the greater the impacts are. Thus, the design system aberration should be as small as possible. Second, low-order astigmatism ($N = 4, 6$) and the Zernike aberrations of those modes whose angular frequency l is not equal to zero and the radial order n that is not equal to the absolute of the angular frequency l have a greater impact. Such aberrations must be corrected first during the design process. Regarding the effect on intensity, an adaptive system must be added to the higher-order photon light sheet microscope to correct the severe effect of aberrations on intensity. According to the effect on thickness, when the light sheet thickness is given priority in designing illuminating light sheets, the higher-order nonlinear excitation has fewer correction items for the adaptive system. This makes the design of the adaptive device more biased for the detection and correction of low-order aberrations. Thus, the number of units of the

adaptive device can be reduced to benefit the design of the adaptive system in the high-order nonlinear multiphoton fluorescent light sheet.

Declaration of competing interest

The authors declare that they have no known competing financial interests or personal relationships that could have appeared to influence the work reported in this paper.

Acknowledgment

This work is supported by the National Natural Science Foundation of China with grant numbers 61805238, 11774342, 31901073 and 11704378.

References

[1] J. Huisken, Optical sectioning deep inside live Embryos by selective plane Illumination Microscopy, Science 305 (5686) (2004) 1007–1009.
[2] P.J. Keller, et al., Reconstruction of Zebrafish early Embryonic development by scanned light sheet microscopy, Science 322 (5904) (2008) 1065–1069.
[3] T.V. Truong, et al., Deep and fast live imaging with two-photon scanned light-sheet microscopy, Nat. Methods 8 (9) (2011) 757–760.
[4] W. Zong, et al., Large-field high-resolution two-photon digital scanned light-sheet microscopy, Cell Res. 25 (2) (2015) 254–257.
[5] R.D. Simmonds, T. Wilson, M.J. Booth, Effects of aberrations and specimen structure in conventional, confocal and two-photon fluorescence microscopy, J. Microsc. 245 (1) (2012) 63–71.
[6] M.J. Booth, Adaptive optical microscopy: the ongoing quest for a perfect image, Light Sci. Appl. 3 (4) (2014) e165.
[7] P. Vermeulen, et al., Adaptive optics for fluorescence wide-field microscopy using spectrally independent guide star and markers, J. Biomed. Opt. 16 (7) (2011) 076019.
[8] X. Tao, et al., Adaptive optics confocal microscopy using direct wavefront sensing, Opt. Lett. 36 (7) (2011) 1062–1064.
[9] M. Booth, et al., Aberrations and adaptive optics in super-resolution microscopy, Microscopy (Oxf) 64 (4) (2015) 251–261.
[10] D. Wilding, et al., Adaptive illumination based on direct wavefront sensing in a light-sheet fluorescence microscope, 24 (22) (2016) 24896.
[11] D. Sinefeld, et al., Adaptive optics in multiphoton microscopy: comparison of two, three and four photon fluorescence, Opt. Express 23 (24) (2015) 31472–31483.
[12] C. Zhang, et al., Analysis of aberrations and performance evaluation of adaptive optics in two-photon light-sheet microscopy, Opt. Commun. 435 (2019) 46–53.
[13] J.W. Goodman, Introduction to Fourier Optics, McGraw-Hill, 1995.
[14] M. Schwertner, M.J. Booth, T. Wilson, Characterizing specimen induced aberrations for high NA adaptive optical microscopy, 12 (26) (2004) 6540.
[15] M. Schwertner, et al., Measurement of specimen-induced aberrations of biological samples using phase stepping interferometry, J. Microsc. 213 (1) (2004) 11–19.
[16] K. Wang, et al., Rapid adaptive optical recovery of optimal resolution over large volumes, Nature Methods 11 (6) (2014) 625–628.
[17] K. Wang, et al., Direct wavefront sensing for high-resolution in vivo imaging in scattering tissue, Nature Commun. 6 (1) (2015) 7276.